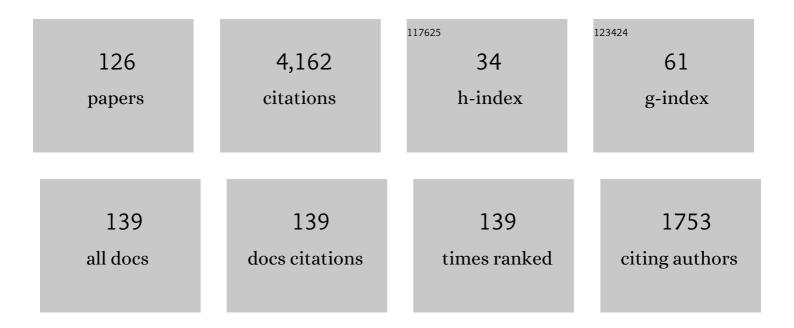
## Anders V Christiansen

List of Publications by Year in descending order

Source: https://exaly.com/author-pdf/396905/publications.pdf Version: 2024-02-01



#	Article	IF	CITATIONS
1	Layered and laterally constrained 2D inversion of resistivity data. Geophysics, 2004, 69, 752-761.	2.6	352
2	Quasi-3D modeling of airborne TEM data by spatially constrained inversion. Geophysics, 2008, 73, F105-F113.	2.6	292
3	An overview of a highly versatile forward and stable inverse algorithm for airborne, ground-based and borehole electromagnetic and electric data. Exploration Geophysics, 2015, 46, 223-235.	1.1	230
4	Piecewise 1D laterally constrained inversion of resistivity data. Geophysical Prospecting, 2005, 53, 497-506.	1.9	224
5	A review of helicopterâ€borne electromagnetic methods for groundwater exploration. Near Surface Geophysics, 2009, 7, 629-646.	1.2	220
6	A global measure for depth of investigation. Geophysics, 2012, 77, WB171-WB177.	2.6	183
7	An integrated processing scheme for high-resolution airborne electromagnetic surveys, the SkyTEM system. Exploration Geophysics, 2009, 40, 184-192.	1.1	169
8	Time-domain-induced polarization: Full-decay forward modeling and 1D laterally constrained inversion of Cole-Cole parameters. Geophysics, 2012, 77, E213-E225.	2.6	108
9	A resolution study of buried valleys using laterally constrained inversion of TEM data. Journal of Applied Geophysics, 2008, 65, 10-20.	2.1	94
10	Resolving spectral information from time domain induced polarization data through 2-D inversion. Geophysical Journal International, 2013, 192, 631-646.	2.4	89
11	Sharp spatially constrained inversion with applications to transient electromagnetic data. Geophysical Prospecting, 2015, 63, 243-255.	1.9	86
12	Groundwater salinity influenced by Holocene seawater trapped in incised valleys in the RedÂRiver delta plain. Nature Geoscience, 2017, 10, 376-381.	12.9	84
13	Detailed landfill leachate plume mapping using 2D and 3D electrical resistivity tomography - with correlation to ionic strength measured in screens. Journal of Applied Geophysics, 2017, 138, 1-8.	2.1	79
14	Mapping of landfills using timeâ€domain spectral induced polarization data: the Eskelund case study. Near Surface Geophysics, 2012, 10, 575-586.	1.2	68
15	Application of time domain induced polarization to the mapping of lithotypes in a landfill site. Hydrology and Earth System Sciences, 2012, 16, 1793-1804.	4.9	66
16	A method for cognitive 3D geological voxel modelling of AEM data. Bulletin of Engineering Geology and the Environment, 2013, 72, 421-432.	3.5	66
17	Laterally constrained inversion of helicopter-borne frequency-domain electromagnetic data. Journal of Applied Geophysics, 2009, 67, 259-268.	2.1	64

18 The transient electromagnetic method. , 2006, , 179-225.

60

#	Article	IF	CITATIONS
19	A Review of Airborne Electromagnetic Methods With Focus on Geotechnical and Hydrological Applications From 2007 to 2017. Advances in Geophysics, 2017, , 47-93.	2.8	59
20	Quantification of modeling errors in airborne TEM caused by inaccurate system description. Geophysics, 2011, 76, F43-F52.	2.6	58
21	Combining 3D geological modelling techniques to address variations in geology, data type and density – An example from Southern Denmark. Computers and Geosciences, 2015, 81, 53-63.	4.2	56
22	Improvement in MRS parameter estimation by joint and laterally constrained inversion of MRS and TEM data. Geophysics, 2012, 77, WB191-WB200.	2.6	49
23	Test-site calibration and validation of airborne and ground-based TEM systems. Geophysics, 2013, 78, E95-E106.	2.6	49
24	Imaging subsurface migration of dissolved CO2 in a shallow aquifer using 3-D time-lapse electrical resistivity tomography. Journal of Applied Geophysics, 2014, 101, 31-41.	2.1	49
25	Origin and extent of fresh groundwater, salty paleowaters and recent saltwater intrusions in Red River flood plain aquifers, Vietnam. Hydrogeology Journal, 2012, 20, 1295-1313.	2.1	47
26	Large-scale 3-D modeling by integration of resistivity models and borehole data through inversion. Hydrology and Earth System Sciences, 2014, 18, 4349-4362.	4.9	47
27	Subsurface imaging of water electrical conductivity, hydraulic permeability and lithology at contaminated sites by induced polarization. Geophysical Journal International, 2018, 213, 770-785.	2.4	47
28	Efficient full decay inversion of MRS data with a stretched-exponential approximation of the distribution. Geophysical Journal International, 2012, 190, 900-912.	2.4	45
29	Direct current (DC) resistivity and induced polarization (IP) monitoring of active layer dynamics at high temporal resolution. Cold Regions Science and Technology, 2015, 119, 16-28.	3.5	45
30	The transient electromagnetic method. , 2009, , 179-226.		43
31	Laterally and Mutually Constrained Inversion of Surface Wave Seismic Data and Resistivity Data. Journal of Environmental and Engineering Geophysics, 2005, 10, 251-262.	0.5	40
32	A quantitative appraisal of airborne and groundâ€based transient electromagnetic (TEM) measurements in Denmark. Geophysics, 2003, 68, 523-534.	2.6	37
33	Integrated management and utilization of hydrogeophysical data on a national scale. Near Surface Geophysics, 2009, 7, 647-659.	1.2	37
34	Processing and inversion of commercial helicopter time-domain electromagnetic data for environmental assessments and geologic and hydrologic mapping. Geophysics, 2013, 78, E149-E159.	2.6	37
35	Three-dimensional geological modelling of AEM resistivity data — A comparison of three methods. Journal of Applied Geophysics, 2015, 115, 65-78.	2.1	36
36	Improved Geoarchaeological Mapping with Electromagnetic Induction Instruments from Dedicated Processing and Inversion. Remote Sensing, 2016, 8, 1022.	4.0	36

#	Article	IF	CITATIONS
37	Mutually and laterally constrained inversion of CVES and TEM data: a case study. Near Surface Geophysics, 2007, 5, 115-123.	1.2	30
38	Compiling a national resistivity atlas of Denmark based on airborne and ground-based transient electromagnetic data. Journal of Applied Geophysics, 2016, 134, 199-209.	2.1	30
39	Performance evaluation of groundwater model hydrostratigraphy from airborne electromagnetic data and lithological borehole logs. Hydrology and Earth System Sciences, 2015, 19, 3875-3890.	4.9	28
40	Hydrostratigraphic modeling using multiple-point statistics and airborne transient electromagnetic methods. Hydrology and Earth System Sciences, 2018, 22, 3351-3373.	4.9	28
41	Accurate quasi 3D versus practical full 3D inversion of AEM data – the Bookpurnong case study. Preview, 2010, 2010, 23-31.	0.1	27
42	A comprehensive study of parameter determination in a joint MRS and TEM data analysis scheme. Near Surface Geophysics, 2013, 11, 557-567.	1.2	27
43	A concept for calculating accumulated clay thickness from borehole lithological logs and resistivity models for nitrate vulnerability assessment. Journal of Applied Geophysics, 2014, 108, 69-77.	2.1	26
44	Field-scale time-domain spectral induced polarization monitoring of geochemical changes induced by injected CO <sub>2</sub> in a shallow aquifer. Geophysics, 2015, 80, WA113-WA126.	2.6	26
45	Time-domain induced polarization – an analysis of Cole–Cole parameter resolution and correlation using Markov Chain Monte Carlo inversion. Geophysical Journal International, 2017, 211, 1341-1353.	2.4	26
46	Data repeatability and acquisition techniques for timeâ€domain spectral induced polarization. Near Surface Geophysics, 2013, 11, 391-406.	1.2	24
47	Field-scale comparison of frequency- and time-domain spectral induced polarization. Geophysical Journal International, 2018, 214, 1441-1466.	2.4	21
48	Airborne and groundâ€based transient electromagnetic mapping of groundwater salinity in the Machile–Zambezi Basin, southwestern Zambia. Near Surface Geophysics, 2015, 13, 383-396.	1.2	20
49	3D characterization of the subsurface redox architecture in complex geological settings. Science of the Total Environment, 2019, 693, 133583.	8.0	20
50	Machine learning based fast forward modelling of ground-based time-domain electromagnetic data. Journal of Applied Geophysics, 2021, 187, 104290.	2.1	18
51	An efficient hybrid scheme for fast and accurate inversion of airborne transient electromagnetic data. Exploration Geophysics, 2016, 47, 323-330.	1.1	16
52	Permeability Estimation Directly From Loggingâ€Whileâ€Drilling Induced Polarization Data. Water Resources Research, 2018, 54, 2851-2870.	4.2	16
53	Combining Clustering Methods With MPS to Estimate Structural Uncertainty for Hydrological Models. Frontiers in Earth Science, 2019, 7, .	1.8	16
54	A discussion of 2D induced polarization effects in airborne electromagnetic and inversion with a robust 1D laterally constrained inversion scheme. Geophysics, 2019, 84, E75-E88.	2.6	16

#	Article	IF	CITATIONS
55	High resolution 3D subsurface mapping using a towed transient electromagnetic system ―tTEM: case studies. Near Surface Geophysics, 2020, 18, 249-259.	1.2	16
56	Soil electrical conductivity imaging using a neural network-based forward solver: Applied to large-scale Bayesian electromagnetic inversion. Journal of Applied Geophysics, 2020, 176, 104012.	2.1	16
57	Utilizing the towed Transient ElectroMagnetic method (tTEM) for achieving unprecedented near-surface detail in geological mapping. Engineering Geology, 2021, 288, 106125.	6.3	16
58	A direct comparison of EMI data and borehole data on a 1000 ha data set. Geoderma, 2017, 303, 188-195.	5.1	14
59	Effect of electrode shape on grounding resistances — Part 2: Experimental results and cryospheric monitoring. Geophysics, 2016, 81, WA169-WA182.	2.6	13
60	Mapping localised freshwater anomalies in the brackish paleo-lake sediments of the Machile–Zambezi Basin with transient electromagnetic sounding, geoelectrical imaging and induced polarisation. Journal of Applied Geophysics, 2015, 123, 81-92.	2.1	12
61	Artificial neural networks for removal of couplings in airborne transient electromagnetic data. Geophysical Prospecting, 2016, 64, 741-752.	1.9	12
62	Contributions to uncertainty related to hydrostratigraphic modeling using multiple-point statistics. Hydrology and Earth System Sciences, 2018, 22, 5485-5508.	4.9	12
63	Geophysicsâ€Based Contaminant Mass Discharge Quantification Downgradient of a Landfill and a Former Pharmaceutical Factory. Water Resources Research, 2018, 54, 5436-5456.	4.2	12
64	A Neural Network-Based Hybrid Framework for Least-Squares Inversion of Transient Electromagnetic Data. IEEE Transactions on Geoscience and Remote Sensing, 2022, 60, 1-10.	6.3	12
65	Resolution of well-known resistivity equivalences by inclusion of time-domain induced polarization data. Geophysics, 2018, 83, E47-E54.	2.6	11
66	3D multiple-point geostatistical simulation of joint subsurface redox and geological architectures. Hydrology and Earth System Sciences, 2021, 25, 2759-2787.	4.9	11
67	Mapping the fresh-saltwater interface in the coastal zone using high-resolution airborne electromagnetics. First Break, 2017, 35, .	0.4	11
68	Presenting a free, highly flexible inversion code. , 2008, , .		10
69	Iterative modelling of AEM data based on a priori information from seismic and borehole data. Near Surface Geophysics, 2014, 12, 635-650.	1.2	10
70	Cross-borehole tomography with full-decay spectral time-domain induced polarization for mapping of potential contaminant flow-paths. Journal of Contaminant Hydrology, 2019, 226, 103523.	3.3	10
71	On-time modelling using system response convolution for improved shallow resolution of the subsurface in airborne TEM. Exploration Geophysics, 2020, 51, 4-13.	1.1	10
72	Effect of Data Pre-Processing on the Performance of Neural Networks for 1-D Transient Electromagnetic Forward Modeling. IEEE Access, 2021, 9, 34635-34646.	4.2	10

#	Article	IF	CITATIONS
73	Optimizing a layered and laterally constrained 2D inversion of resistivity data using Broyden's update and 1D derivatives. Journal of Applied Geophysics, 2004, 56, 247-261.	2.1	10
74	Experience from Two Resistivity Inversion Techniques Applied in Three Cases of Geotechnical Site Investigation. Journal of Geotechnical and Geoenvironmental Engineering - ASCE, 2008, 134, 1730-1742.	3.0	9
75	A Regional Scale Hydrostratigraphy Generated from Geophysical Data of Varying Age, Type, and Quality. Water Resources Management, 2019, 33, 539-553.	3.9	9
76	Processing and inversion of SkyTEM data for high resolution hydrogeophysical surveys. ASEG Extended Abstracts, 2007, 2007, 1-4.	0.1	8
77	On the value of including x-component data in 1D modeling of electromagnetic data from helicopterborne time domain systems in horizontally layered environments. Journal of Applied Geophysics, 2012, 84, 61-69.	2.1	8
78	AEMIP robust inversion using maximum phase angle Cole–Cole model re-parameterisation applied for HTEM survey over Lamego gold mine, QuadrilÃįtero FerrÃfero, MG, Brazil. Exploration Geophysics, 2020, 51, 170-183.	1.1	8
79	Crossâ€borehole geoelectrical timeâ€lapse monitoring of in situ chemical oxidation and permeability estimation through induced polarization. Near Surface Geophysics, 2021, 19, 43-58.	1.2	8
80	Sampling density and spatial analysis: a methodological pXRF study of the geochemistry of a Viking-Age house in Ribe, Denmark. Archaeological and Anthropological Sciences, 2021, 13, 1.	1.8	8
81	Airborne Transient EM Methods and Their Applications for Coastal Groundwater Investigations. Coastal Research Library, 2013, , 121-153.	0.4	7
82	Constrained inversion of IP parameters from Airborne EM data. ASEG Extended Abstracts, 2013, 2013, 1-4.	0.1	7
83	Successful Sampling Strategy Advances Laboratory Studies of NMR Logging in Unconsolidated Aquifers. Geophysical Research Letters, 2017, 44, 11,021.	4.0	7
84	Anthropogenic wetlands due to over-irrigation of desert areas: a challenging hydrogeological investigation with extensive geophysical input from TEM and MRS measurements. Hydrology and Earth System Sciences, 2017, 21, 1527-1545.	4.9	7
85	An efficient 2D inversion scheme for airborne frequency-domain data. Geophysics, 2018, 83, E189-E201.	2.6	7
86	Search and recovery of aircraft parts in ice-sheet crevasse fields using airborne and in situ geophysical sensors. Journal of Glaciology, 2020, 66, 496-508.	2.2	7
87	tTEM20AAR: a benchmark geophysical data set for unconsolidated fluvioglacial sediments. Earth System Science Data, 2021, 13, 2743-2752.	9.9	5
88	Efficient Reduction of Powerline Signals in Magnetic Data Acquired From a Moving Platform. IEEE Transactions on Geoscience and Remote Sensing, 2021, 59, 7137-7146.	6.3	5
89	Application of 2D laterally constrained inversion and 2D smooth inversion of CVES resistivity data in a slope stability investigation. , 2003, , .		5
90	Accelerated 2.5-D inversion of airborne transient electromagnetic data using reduced 3-D meshing. Geophysical Journal International, 2022, 230, 643-653.	2.4	5

ANDERS V CHRISTIANSEN

1

#	Article	IF	CITATIONS
91	Reliability of Time Domain Induced Polarization Data. , 2011, , .		4
92	Utilizing massively parallel co-processors in the AarhusInv 1D forward and inverse AEM modelling code. ASEG Extended Abstracts, 2015, 2015, 1-3.	0.1	4
93	Layered 2-D inversion of profile data, evaluated using stochastic models. ASEG Extended Abstracts, 2003, 2003, 1-8.	0.1	4
94	A parallel computing thinâ€sheet inversion algorithm for airborne timeâ€domain data utilising a variable overburden. Geophysical Prospecting, 2018, 66, 1402-1414.	1.9	3
95	Using geophysical survey results in the inference of aquifer vulnerability measures. Near Surface Geophysics, 2021, 19, 505-521.	1.2	2
96	Optimising geological mapping of glacial deposits using high-resolution electromagnetic induction data. Geological Survey of Denmark and Greenland Bulletin, 0, , 9-12.	2.0	2
97	The Use of Airborne Electromagnetic Systems for Hydrogeological Investigations. , 2000, , .		2
98	Spatially Constrained Inversion for Quasi 3D Modeling of AEM Data. , 2008, , .		2
99	STRUCTURAL MAPPING OF LARGE AQUIFER STRUCTURES. , 2006, , .		2
100	Integrating neural networks in least-squares inversion of airborne time-domain electromagnetic data. Geophysics, 2022, 87, E177-E187.	2.6	2
101	Fast 2.5D and 3D inversion of transient electromagnetic surveys using the octree-based finite-element method. Geophysics, 2022, 87, E267-E277.	2.6	2
102	Technical note: Efficient imaging of hydrological units below lakes and fjords with a floating, transient electromagneticÂ(FloaTEM) system. Hydrology and Earth System Sciences, 2022, 26, 2813-2827.	4.9	2
103	Overly steep decays in airborne TEM data and their link to chargeability: example from the Howards East District, NT, Australia. ASEG Extended Abstracts, 2019, 2019, 1-5.	0.1	1
104	Towards 3D inversion of ground based TEM data. ASEG Extended Abstracts, 2016, 2016, 1-5.	0.1	1
105	Quasi 3â€Ð inversion of electromagnetic data. , 2008, , .		1
106	FROM RESISTIVITY TO CLAY THICKNESS $\hat{a} \in \hat{A}$ AN INVERSION APPROACH. , 2006, , .		1
107	Increased Accuracy in Mineral and Hydrogeophysical Modelling of HTEM Data via Detailed Description of System Transfer Function and Constrained Inversion. , 2009, , .		1

108 The sensitivity functions of TEM methods. , 2000, , .

#	Article	IF	CITATIONS
109	Structural Mapping of Large Aquifer Structures. , 2006, , .		1
110	2-D Laterally constrained inversion (LCI) of resistivity data. , 2002, , .		1
111	Optimizing the 2D laterally constrained inversion (2D-LCI) using a Quasi-Newton method and 1D derivatives. , 2003, , .		1
112	Spatially Constrained Inversion of Area Covering Datasets. , 2006, , .		1
113	Non-destructive 3D prospection at the Viking Age fortress Borgring, Denmark. Journal of Archaeological Science: Reports, 2022, 42, 103351.	0.5	1
114	Mapping Aquifer Vulnerability. , 2006, , .		0
115	Quasi-3D inversion of full size AEM datasets. ASEG Extended Abstracts, 2015, 2015, 1-3.	0.1	Ο
116	Geostatistical analysis of the relationship between airborne electromagnetic data and borehole lithological data. ASEG Extended Abstracts, 2015, 2015, 1-4.	0.1	0
117	Effective and accurate processing electromagnetic data and inversion of airborne. ASEG Extended Abstracts, 2016, 2016, 1-3.	0.1	0
118	ANTHROPOGENIC WETLANDS DUE TO OVER-IRRIGATION OF DESERT AREAS; A CHALLENGING HYDROGEOLOGICAL INVESTIGATION WITH EXTENSIVE GEOPHYSICAL INPUT FROM TEM AND MRS MEASUREMENTS. , 2016, , .		0
119	Why Not X in Airborne TEM?. , 2006, , .		0
120	Spatially Constrained Inversion for Quasi 3-D Modelling of AEM Data. ASEG Extended Abstracts, 2007, 2007, 1-4.	0.1	0
121	Employing Airborne Electromagnetics for Spatial and Temporal Hydrogeophysical Monitoring: A View from Opposite Ends of the Globe. , 2011, , .		0
122	Mapping Soil Heterogeneity Using Spatially Constrained Inversion of Electromagnetic Induction Data. , 2015, , .		0
123	Compilation of a Resistivity Atlas of Danish lithologies based on direct resistivity measurements and wireline logging data. ASEG Extended Abstracts, 2015, 2015, 1-4.	0.1	0
124	Quantifying the effect of primary field modelling on TEMPEST data - The importance of uncertainty. ASEG Extended Abstracts, 2016, 2016, 1-5.	0.1	0
125	Creating 3D images of the subsurface from high-resolution towed transient electromagnetic data. , 2018, , .		0
126	A towed magnetic gradiometer array for rapid, detailed imaging of utility, geological, and archaeological targets. Geoscientific Instrumentation, Methods and Data Systems, 2021, 10, 313-323.	1.6	0